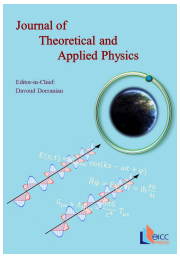

Volume 17, Issue 1, 172303 (1-6)

Journal of Theoretical and Applied Physics (JTAP)

https://dx.doi.org/10.57647/j.jtap.2023.1701.03

THz generation by a periodic array of a photoconductive antenna of GaAs material in the presence of a magnetic field

Sandeep Sandeep[1,2], Hitendra K. Malik[1]*

[1]*Plasma Science and Technology Laboratory, Department of Physics, Indian Institute of Technology Delhi, New Delhi, India.*
[2]*Department of Physics, Deen Dayal Upadhyaya College, University of Delhi, New Delhi, India.*

***Corresponding author**: hkmalik1970@gmail.com

Received 29 October 2022; Accepted 8 December 2022; Published online 12 December 2022

Abstract:
Terahertz radiation finds applications in medical science, spectroscopy, security screening, communication, etc. There are several methods that focus on the interaction of lasers with plasma, and laser beating process is an effective scheme for the Terahertz radiation generation. In this scheme, a resonance between the beating frequency and plasma frequency needs to be achieved. In general, only the plasma electrons respond to the lasers field. However, achieving a Terahertz source with variable frequency and power is very difficult, even with the application of an external magnetic field. In this article, we give an analytical analysis of how employing an external magnetic field, a laser-induced transient current in an array of GaAs structures can be used to increase the power of the emitted radiation. The magnetic field has the benefit of not stopping the carriers since these gyrate before they reached the corner, which causes the frequency to affect the current and helps lasting this interaction for a longer time. As a result, 2-3 cycles of the higher frequency pulse are generated, increasing the power by 100 times.

Keywords: Strong magnetic field; Heavy qurakonium; Fractional Schrödinger equation

1. Introduction

Although various methods have been proposed to increase the power, the radiated power of the Terahertz radiation remains very low. Different methods have been utilized to enhance the radiation power from a PCA (Photoconductive Antenna), such as by using different antenna geometries, different semiconductor materials, and collimating lenses [1–6]. Even after utilizing different methods as mentioned previously, the efficiency of the PCA remains very low. Although some theoretical, experimental, and simulation studies [7–9] have been performed to improve the radiation from the PCA, the radiated power needs to be worked out for its enhancement.

Prajapati et al. [10, 11] have shown that the net electric field at the electrode gap is adversely affected by the radiated near-zone field, which is reflected in the PCA as a decreased current density. The intensity of the far-zone electric field is radiated and decreases with the current density because it is proportional to the rate at which the current density changes. In addition to mitigating the loss in current density caused by the radiated near-zone electric field, it is feasible to increase PCA radiation with the help of an external magnetic field. The fact that the polarity of the radiated far-zone electric field can also be controlled by the orientation of the applied external magnetic field is further evidence that the radiated field on big aperture PCA is amplified in the presence of an external magnetic field. Therefore, the radiation intensity can be boosted by utilizing an external magnetic field to reduce the near-zone field effect.

In order to effectively contribute to terahertz radiation, the transit time of the photocarriers to the photoconductor contact electrodes must be within a fraction of the terahertz oscillation period. Yang et al. [12] demonstrated the 7.5% optical-to-terahertz power conversion efficiency in experiments. At a 1.4 mW optical pump, 10^5 W of wideband terahertz radiation with a frequency range of 0.1-2 THz

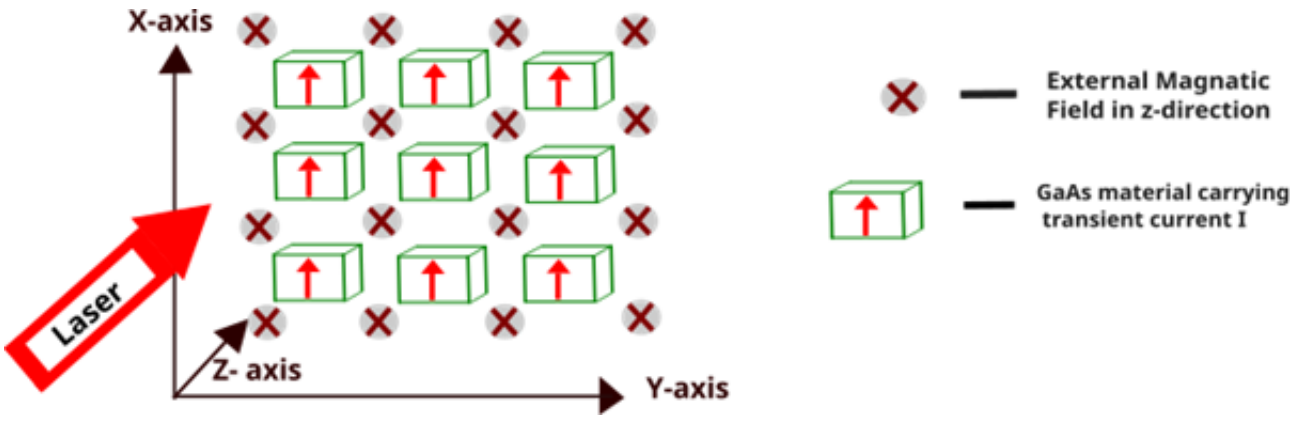

Figure 1. Schematic of THz emission from a periodic array of photoconductive antenna exposed to a laser in the presence of a magnetic field.

has been produced. To boost power efficiency and boost optical-to-terahertz conversion efficiencies, larger device active areas, better aspect ratios, and three-dimensional plasmonic contact electrodes have been suggested to be employed [13, 14].

Singh et al. [15] experimentally demonstrated photoconductive emitters (PCEs) based on SI-GaAs that have used carbon irradiated (10^{14} ions/cm^2) up to 2 μm deep for producing THz pulses with an increase in power of about 100 times and an efficiency of electrical to THz power conversion of 800 times higher than PCEs on SI-GaAs that are typically used. The SI-GaAs substrate was irradiated, which resulted in many defects and a shorter lifetime for photo-excited carriers. Depending on the irradiation dose, a reduction in the total current flowing through the substrate was found to cause a corresponding reduction in heat dissipation in the device. Due to this, the maximum cut-off applied voltage across PCE electrodes to run the device without thermal breakdown has increased from $\sim$ 35 V to $>$ 150 V for the 25 μm electrode gaps.

When the laser is incident on GaAs material, the carriers are formed with zero current and due to biased voltage the current will reach a maximum finite value and at the same time the carriers reach the sample's corner, where the carriers stop. Before they halt, the carrier has a larger current density than at the rear, and the field that is generated is the self-consistent electric field owing to the near-field effect. This field is opposite to the applied biased field but has a higher magnitude than the biased voltage. This transient current will only create one or a half cycle of THz, which may lengthen the duration of the THz. Due to the fact that the magnetic field does not stop the carriers but instead spin them before they reach the corner, the frequency will have an effect on the current, and the current will remain for an extended amount of time. So, the pulse of higher frequency and of 2-3 cycles will be generated. The power can be small, but it will continue for a long while. Considering this, the total current density is a superposition of current densities due to the biased field and the current density due to internal THz near field. In the present work, we have demonstrated this mechanism using the periodic array of a photoconductive antenna of GaAs material in the presence of a magnetic field.

2. Current density due to photoconductive antenna

In this section, we find the current density due to the transient current produced by the photoconductive antenna in the manifestation of laser in the presence of electric and magnetic field. We consider a planar array of antennae along the $\hat{z}$ - direction with centre at $(m_1 d, m_2 d)$ such that

$$m_1 = 0, 1, 2, - - - - - - - -M_1$$

$$m_2 = 0, 1, 2, - - - - - - - -M_2$$

Each alternating GaAs gap is an antenna at $(m_1\hat{x}, m_2\hat{z})d$ acting as an oscillatory dipole with oscillating dipole height $dl\hat{x}$ and current I, so that

$$I(t)dl\hat{x} = \mathbf{J}(t)bld$$

Figure 1 shows a schematic illustration of the photoconductive antenna array. Every photoconductive antenna's two sets of metal electrodes are centred by an LT-GaAs gap in the presence of electric and magnetic fields. The magnetic field is taken along the z-axis and the biased voltage is along the x-axis.

Considering the photoconductive electron of mass m with velocity $\mathbf{v}$ under a dc bias electric field ($\mathbf{E}$) and external magnetic field $\mathbf{B}$, the equation of motion reads

$$m\frac{d\mathbf{v}}{dt} = -e\mathbf{E} - m\mathbf{v}\nu - e\mathbf{v}\times\mathbf{B} \tag{1}$$

where ω_c is the cyclotron frequency at which the electron will gyrate when there is a magnetic field and ν is the collisional frequency. The x-component of the Eq. (1)

$$\frac{dv_x}{dt} + \nu v_x + \omega_c v_y = 0 \tag{2}$$

The y-component of the Eq. (1),

$$\frac{dv_y}{dt} + \nu v_y + \omega_c v_x = -i\frac{eE_0}{m} \tag{3}$$

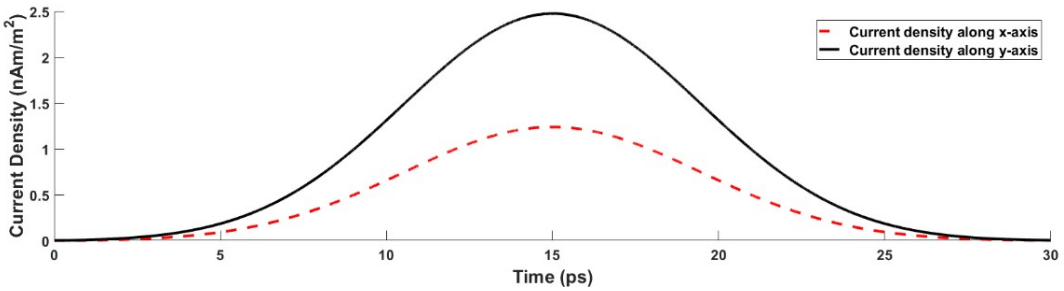

Figure 2. Current density plot in time domain along y and x axis for α= 0.5

Equation (2) and equation (3) are added, and the resultant is integrated to get

$$(v_x + iv_y) = -i\frac{eE_0}{m}\left(\frac{1}{\acute{\nu}} - \frac{e^{-\acute{\nu}t}}{\acute{\nu}}\right) \tag{4}$$

where $\acute{\nu} = (\nu - i\omega c)$.
Equation (2) and equation (3) are subtracted, and the resultant is integrated to get

$$(v_x - iv_y) = i\frac{eE_0}{m}\left(\frac{1}{\acute{\acute{\nu}}} - \frac{e^{-\acute{\acute{\nu}}t}}{\acute{\acute{\nu}}}\right) \tag{5}$$

where, $\acute{\acute{\nu}} = (\nu + i\omega_c)$. Finding the v_x by adding equation (4) and (5),

$$v_x = i\frac{eE_0}{m(\nu^2+\omega_c^2)}[-i\omega_c + i\nu e^{-\nu t}\sin(\omega_c t) + i\omega_c e^{-\nu t}\cos(\omega_c t)] \tag{6}$$

Finding the v_y by subtracting equation (4) and (5),

$$v_y = i\frac{-eE_0}{m(\nu^2+\omega_c^2)}[\nu - \nu e^{-\nu t}\cos(\omega_c t) + \omega_c e^{-\nu t}\sin(\omega_c t)] \tag{7}$$

These relations are used in the current density $\mathbf{J}(t) = en(t)\mathbf{v}$. The x- and y-components of the current density $\mathbf{J}(t)$ yield

$$J_x(t) = \frac{n(t)e^2E_0}{m(\nu^2+\omega_c^2)}[\omega_c - \nu e^{-\nu t}\sin(\omega_c t) - \omega_c e^{-\nu t}\cos(\omega_c t)] \tag{8}$$

$$J_y(t) = \frac{n(t)e^2E_0}{m(\nu^2+\omega_c^2)}[\nu - \nu e^{-\nu t}\cos(\omega_c t) - \omega_c e^{-\nu t}\sin(\omega_c t)] \tag{9}$$

For typical parameters, $\nu = 10^{12}\text{s}^{-1}$, $\omega_c = \alpha\nu$ and E_0= 20 KV/m and taking different values of α= 0.1,0.2,1; $t = t_p \times 10^{12}$ sec, we get

$$J_y(t_p) = 8.4\times10^{-27}\frac{n(t_p)}{(1+\alpha^2)}[1 - e^{-t_p}\sin(\alpha t_p) - \alpha e^{-t_p}\sin(\alpha t_p)] \tag{10}$$

The Fourier transformation of which is calculated using the following formula

$$\mathbf{J}_\omega = \frac{1}{\sqrt{2\pi}}\int_{-\infty}^{\infty} e^{i\omega t}dt$$

In order to solve the problem, numerical solution is followed. It is worth mentioning that the numerical methods

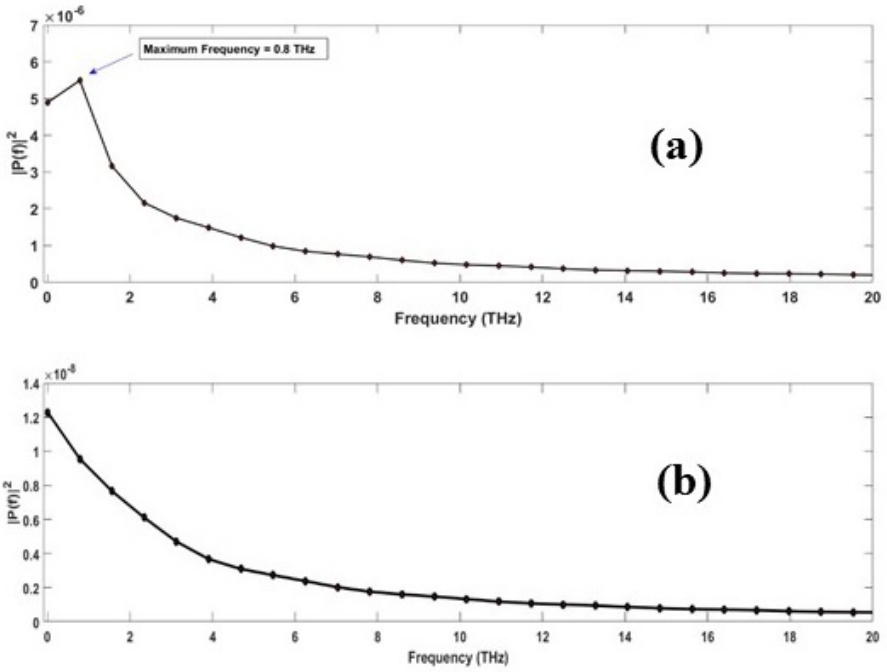

Figure 3. Current density plot in frequency domain along y-direction (a) and along x-direction (b).

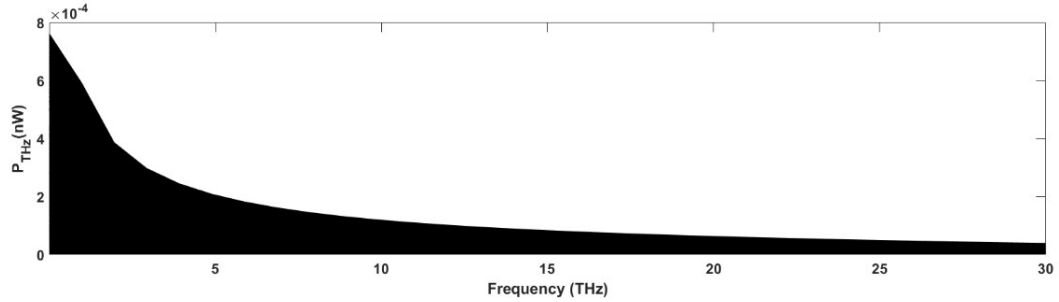

Figure 4. THz power (nW) radiated in the x-direction versus frequency, when l= 3 μm, d= 0.8 μm, b= 1 μm, μ= 2.62, ϑ= 10^{12} s^{-1}, E_b= 20 kV/cm, M_1= 50, and M_2= 20.

have proved their significance in other field as well [14–17]. The current densities obtained in the x- and y-directions are plotted in Fig. 2. This can be observed that there is a larger difference in the magnitude of these currents. This can be explained as followed. Since the external magnetic field is in the z-direction, the Lorenz force is zero in the direction of the field and is greatest in directions perpendicular to the external field in the x-y plane. The biased voltage in the x-direction has been applied, which has much significant impact on the current density. In view of this, the current along the x-direction is insignificantly affected by the magnetic field while in the y-direction the current is 2.5 times larger for the typical parameters of collision frequency ν=10^{12}s^{-1}, cyclotron frequency ω_c=0.5×10^{12}s^{-1} and biased voltage E_0=20 kV/m.

In Fig. 3(a), the variation of the current density that has been Fourier transformed, i.e. the current density in the frequency domain, is depicted. Here this is seen that the maximum current is achieved at about 0.8 THz frequency. On the other hand, Fig. 3(b) demonstrates that the current density in the frequency domain has insignificantly lower current along the y-axis.

It is clear that the THz radiation at the frequency of 0.8 THz would be significantly achievable in the current mechanism and it will be possible to control its peak value controlled by the electron density of the photoconductive antenna because the profile of the emitted THz radiation in general remains in accord with the profile of the nonlinear current [16, 17]. Additionally, the fast rise and slow decrease of the density in this process is consistent to the finding Darrow et al. [18] for large-aperture photoconductive antennae. Numerous other disciplines likewise make use of numerical math of a similar nature [19, 20].

The fast rise and slow decrease of the density in the present mechanism can be understood as follows. The laser is incident in the direction normal to the GaAs material having band gap E_g. The laser field is taken to be Gaussian as $E_L^2(t) = E_{L0}^2 \exp[-(t-t_0)^2/\tau^2]$, where E_{L0} is the amplitude of the field. τ is taken to be called the laser's pulse duration and t_0 corresponds to the retarded time. Now the laser radiation results free electron production (density n_e) from the valence band at the rate of $\partial n_e/\partial t = R$, where

$$R = \frac{2\omega}{9\pi^2}\left(\frac{m\omega}{\hbar}\right)^{\frac{3}{2}}\Gamma^{-\frac{5}{2}} e^{\frac{-\pi E_g \Gamma}{2\hbar\omega}} \tag{11}$$

together with $\Gamma = (16/e_0)(me_g/m_0)^{1/2}$.

We discuss the situation with strong field, i.e., when $\Gamma < 1$. In the above equation, e_0 is E_0 in units of 10^4 esu, e_g is the band gap in units of eV, m_0 is the electron mass in free space and m is its effective mass in the material. If the laser intensity is 10^{14} W/cm^2, laser pulse duration is 25 fs, $\omega = 2\times10^{15}$ rad s^{-1}, then R (in cm^{-3} s^{-1}) can be obtained from the above relations as

$$R = 4\times10^{33}\left(\frac{m}{m_0}\right)^{\frac{1}{4}}\left(\frac{e_g}{e_0^2}\right)^{-\frac{5}{4}} e^{\left(-20(\frac{meg}{m_0 e_0^2})^{\frac{1}{2}}\right)} \tag{12}$$

After trapping time, the electron-hole (e-h) recombine, and the recombination rate is proportional to n_e^2. Hence

$$\frac{\partial n_e}{\partial t} = -\beta n_e^2 \tag{13}$$

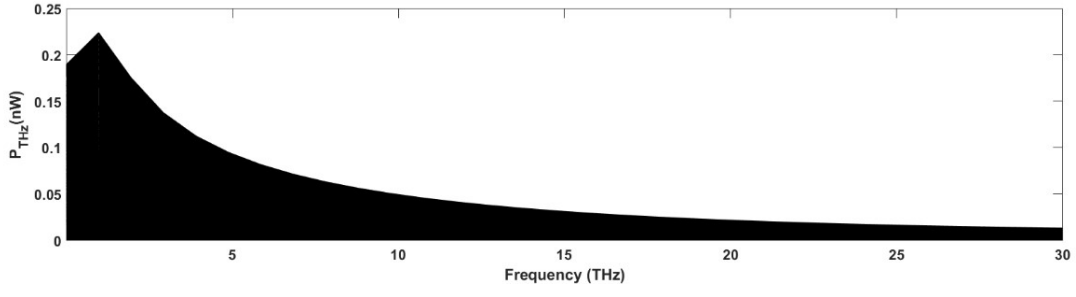

Figure 5. THz power (nW) radiated in the y-direction versus frequency, when l= 3 μm, d= 0.8 μm, b= 1 μm, μ= 2.62, ϑ= 10^{12} s^{-1}, E_b= 20 kV/cm, M_1= 50, and M_2= 20.

where β is the recombination constant. The integration of the above equation reads

$$-\frac{1}{n_e} = -\beta t - \frac{1}{n_{e0}} \tag{14}$$

where n_{e0}= 10^{18} cm^{-3} is the carrier density when recombination starts and β= 10^{11} cm^{-3} s^{-1}. From this, we can arrange to get

$$n_e = \frac{n_{e0}}{1+n_{e0}\beta t} \tag{15}$$

Therefore, the equation governing the net electron density is written as,

$$\frac{\partial n_e}{\partial t} = R - \beta n_e^2 \tag{16}$$

The rise and slow decrease of the density is depending upon R and β, respectively. In discussing the same, we have assumed the laser field to be Gaussian. However, there are additional laser beam profiles available that have established their significance in the field of optics [21–24].

3. Radiated THz power

Following Kumar et al. [25], the average power per unit solid angle in (θ,ϕ) plane due to $\mathbf{J}(t)$ can be evaluated as

$$P_{THz} = 4\pi\frac{c}{2\mu_0}\left(\frac{\omega}{c}\frac{\mu_0}{4\pi}\frac{(|\mathbf{J}(t)|bld)}{r}\right)^2 G(\cos^2\theta+\sin^2\theta\sin^2\phi) \tag{17}$$

where b and l are the breath and length of GaAs gap array,

$$G = \left(\frac{\sin(\frac{M_1\psi_1}{2})\sin(\frac{M_2\psi_2}{2})}{\sin\frac{\psi_1}{2}\sin\frac{\psi_2}{2}}\right)^2,$$

$$\psi_1 = -\frac{bd}{c}\sin\theta\cos\phi = p_1\pi \text{ and } \psi_2 = -\frac{bd}{c}\sin\theta = p_2\pi.$$

Corresponding to the current densities in the x- and y-directions through Eqs. (8) and (9), we can evaluate the power radiated using the Eq. (17). Figure 4 shows the variation of the emitted power in the x-direction, whereas the power radiated by the current density in the y-direction is depicted in Fig. 5. A clear cut enhanced amount of the power of more than 100 times is observed in the y-direction. Consistent to the maximum current at 0.8 THz, the radiated power is also highest at this frequency. Since the current densities show their dependence on the magnetic field, as observed by other investigators also in the case of plasma-based THz emitters [26–32], the present mechanism also consistently follows the similar trend of the emitted power under the impact of external magnetic field.

Finally, we can discuss the physics behind the dependence of the radiated power on the transient current density and the recombination rate of electron-hole pairs. When the laser strikes a GaAs material, the carriers are formed, and when a bias voltage is applied, the carriers begin oscillating and a current is created gradually. If just one current is generated in the sample, the whole antenna functions as a dipole antenna. However, the difficulty with dipole antennas is the short length of the dipole relative to the incident wavelength. Since we are interested in THz and the wavelength is around 100 microns, the 1 cm-long GaAs sample carrying the current is anticipated to function as an antenna for many thousand wavelengths. Nevertheless, this is not wanted. The power will rise in a certain direction if the wire is segmented, which may be accomplished by separating the sample into tiny pieces with each gap measuring less than 100 microns in order to realize them as dipoles. When the laser is incident on a GaAs material, the carrier is created, and the carriers generate current by following the electric field. The time-varying current is induced in a brief time span of recombination time. The evolution of the transient can also be understood in the following manner also. When the femtosecond laser pulse is incident normally to the photoconductive layer of the antenna, the electron–hole pairs are generated within the photoconductive gap of the antenna. This happens because of the higher photon energy of laser pulse in comparison with the band-gap energy of the photoconductive material. When a biased electric field (E_{bias}) is applied across the antenna electrodes through transmission lines, then the photo-excited carriers get accelerated. A macroscopic electron-hole field (E_{e-h}) gets created in the reverse direction because of the physical separation of the charges. As more of electron–hole pairs are generated, there is also an increase in the electron-hole field and after some time the total electric field at the location of carriers near the dipole electrodes (defined as $E_{feld} = E_{bias}$-E_{e-h}) is screened. This results in the reduction of the effective electric field across the photoconductive gap of the antenna. Due to the sudden change in the total electric field, there is a creation of the transient current, which is responsible for the THz radiations from the photoconductive antenna [33]. The generated transient current decays with time constant, which is determined from the carrier lifetime in the photoconductive substrate used for the antenna.

4. Conclusion

We have discussed a scheme of THz radiation generation where a short pulse laser propagates through a periodic array of photoconductive antennae of GaAs material. Across photoconductive antenna there is a nonlinear transient current of picosecond duration excited in direction perpendicular to the direction of the incident laser beam. This nonlinear current acts as phase array dipole antennae, which results in the emission of THz radiation generation. From analysis, it has been observed thar emission of the THz radiation pulses with fast rise and slow fall is easily achievable with maximum power of 0.013 nW at 0.8 THz frequency. The radiated power depends on the transient current density, for which recombination rate of electron-hole pairs plays a vital role. An important role of the external magnetic field results in the enhancement of THz power by around 100 times of the theoretical observed value.

Conflict of interest statement

The authors declare that they have no conflict of interest.

References

[1] H. K. Malik. *Laser-Matter Interaction for Radiation and Energy*. CRC Press, 1th edition, 2021.

[2] A. Dreyhaupt, S. Winnerl, T. Dekorsy, and M. Helm. *Applied Physics Letters*, **86**:121114, 2005.

[3] R. Yano, H. Gotoha, Y. Hirayama, S. Miyashita, Y. Kadoya, and T. Hattori. *Journal of Applied Physics*, **97**:103103, 2005.

[4] M. R. Stone, M. Naftalya, R. E. Miles, J. R. Fletcher, and D. P. Steenson. *IEEE Transactions on Microwave Theory and Techniques*, **52**:2420, 2004.

[5] E. Castro-Camus, J. Lloyd-Hughes, and M. B. Johnston. *Physical Review B*, **71**:195301, 2005.

[6] T. Hattori, K. Egawa, S. I. Ookuma, and T. Itatani. *Japanese Journal of Applied Physics*, **45**:L422, 2006.

[7] G. C. Loata, M. D. Thomson, T. L¨offler, and H. G. Roskos. *Applied Physics Letters*, **91**:232506, 2007.

[8] J. Y. Suen, W. Li, Z. D. Taylor, and E. R. Brown. *Applied Physics Letters*, **96**:141103, 2010.

[9] C. W. Berry and M. Jarrahi. *New Journal of Physics*, **14**:105029, 2012.

[10] J Prajapati, M Bharadwaj, A Chatterjee, and R. Bhattacharjee. *Optics Communications*, **394**:69, 2017.

[11] M. B. Johnston, D. M. Whittaker, A. Corchia, A. G. Davies, and E. H. Linfield. *Physical Review B*, **65**:165301, 2002.

[12] S. H. Yang, M. R. Hashemi, C. W. Berry, and M. Jarrahi. *IEEE Transactions on Terahertz Science and Technology*, **4**:575, 2014.

[13] T. Hattori, K. Egawa, S. I. Ookuma, and T. Itatani. *Japanese Journal of Applied Physics*, **45**:L422, 2006.

[14] A. Dreyhaupt, S. Winnerl, T. Dekorsy, and M. Helm. *Applied Physics Letters*, **86**:121114, 2005.

[15] A. Singh, S. Pal, H. Surdi, S. S. Prabhu, V. Nanal, and R. G. Pillay. *Applied Physics Letters*, **104**:063501, 2014.

[16] H. K. Malik. *Physics Letters A*, **379**:2826, 2015.

[17] H. K. Malik, T. Punia, and D. Sharma. *Electronics*, **10**:3134, 2021.

[18] J. T. Darrow, X. C. Zhang, D. H. Auston, and J. D. Morse. *IEEE Journal of Quantum Electronics*, **28**:1607, 1992.

[19] L. Malik, S. Rawat, M. Kumar, and A. Tevatia. *Materials Today: Proceedings*, **38**:191, 2021.

[20] L. Malik and A. Tevatia. *Defence Science Journal*, **71**:137, 2021.

[21] L. Malik. *Optics and Laser Technology*, **132**:106485, 2020.

[22] L. Malik and A. Escarguel. *Europhysics Letters*, **124**:64002, 2019.

[23] L. Malik, A. Escarguel, M. Kumar, A. Tevatia, and R. S. Sirohi. *Laser Physics Letters*, **18**:086003, 2021.

[24] R. Gill, D. Singh, and H. K. Malik. *Journal of Theoretical and Applied Physics*, **11**:103, 2017.

[25] A. Kumar and P. Kumar. *Physics of Plasmas*, **23**:103302, 2016.

[26] H. K. Malik. *Physics Letters A*, **384**:126304, 2020.

[27] A. K. Malik and H. K. Malik. *IEEE Journal of Quantum Electronics*, **49**:232, 2013.

[28] H. K. Malik and A. K. Malik. *Applied Physics Letters*, **99**:251101, 2011.

[29] A. K. Malik, H. K. Malik, and U. Stroth. *Physical Review E*, **85**:016401, 2012.

[30] D. Singh and H. K. Malik. *Physics of Plasmas*, **21**:083105, 2014.

[31] H. K. Malik and S. Punia. *Physics of Plasmas*, **26**:063102, 2019.

[32] H. K. Malik and R. Gill. *Physics Letters A.*, **382**:2715, 2018.

[33] N. Khiabani, Y. Huang, and Y.-C. Shen. *Proceedings of the 5th European Conference on Antennas and Propagation (EUCAP)*, :462, 2011.